Cell-Penetrating Peptides

DOI: 10.1002/anie.200704444

HIV TAT Forms Pores in Membranes by Inducing Saddle-Splay Curvature: Potential Role of Bidentate Hydrogen Bonding**

*Abhijit Mishra, Vernita D. Gordon, Lihua Yang, Robert Coridan, and Gerard C. L. Wong**

The TAT protein transduction domain (PTD) of the human immunodeficiency virus (HIV-1) can cross cell membranes with unusual efficiency[1] and has many potential biotechnological applications.[2–4] Extant work has provided important clues to the molecular mechanism underlying the activity of this peptide, which consists of 11 amino acids, 8 of which are cationic and 6 of these are arginines. TAT PTD synthesized with D-amino acids enters cells as efficiently as the native form,[5] thereby indicating that the mechanism of transduction is receptor independent; this conclusion is consistent with recent results that suggest that the TAT PTD may enter cells through receptor-independent macropinocytosis.[6] Substitution of any of the PTD's cationic residues with neutral alanine decreases activity, while substitution of neutral residues has no effect.[5] This indicates the importance of electrostatic interactions between cationic TAT PTD and anionic phospholipid membranes. Recent work has shown that the physics of electrostatic interactions can drive a rich polymorphism of self-assembled structures that depend on parameters such as charge density[7,8] and intrinsic membrane curvature.[9,10] However, although arginine-rich polycations can enter cells, cationic polylysine cannot.[11] This shows that electrostatic interactions alone are insufficient for PTD activity and that the arginine residues play a specific, essential role.

We use confocal microscopy and synchrotron X-ray scattering (SAXS) to study the interaction of the TAT PTD with model membranes at room temperature. We find that the transduction activity correlates with induction of negative Gaussian ("saddle-splay") membrane curvature, which is topologically required for pore formation. Moreover, we show that the TAT PTD can drastically remodel vesicles into a porous bicontinuous phase with analogues in block-copolymer systems,[12–14] and we propose a geometric mechanism facilitated by both electrostatics and bidentate hydrogen bonding. The latter is possible for the TAT PTD but not for similarly cationic, nonarginated polypeptides.

Cell membranes are composed of lipids that have fundamentally different interactions with cationic macroions such as TAT PTD. We examine representative model membranes composed of lipids with different charges and intrinsic curvatures: 1,2-dioleoyl-*sn*-glycero-3-phosphocholine (DOPC) and 1,2-dioleoyl-*sn*-glycero-3-phosphoethanolamine (DOPE) have zwitterionic headgroups, while 1,2-dioleoyl-*sn*-glycero-3-[phospho-L-serine] (sodium salt) (DOPS) and 1,2-dioleoyl-*sn*-glycero-3-[phospho-*rac*-(1-glycerol)] (sodium salt) (DOPG) have anionic headgroups; all have zero intrinsic curvature[15] ($C_0 = 0$, "cylinder-shaped") except for DOPE, which has negative intrinsic curvature ($C_0 < 0$, "cone-shaped"). When rhodamine-tagged TAT PTD (Rh-PTD) is applied to the exterior of giant unilamellar vesicles (GUVs, diameters of 5–30 μm) with low DOPE content (0 and 20%), rhodamine fluorescence is seen only outside the GUVs (Figure 1a), thereby indicating that the Rh-PTD has not crossed these membranes. However, when Rh-PTD is applied to GUVs with 40% DOPE content, the rhodamine intensity equilibrates across the membrane over tens of seconds (Figure 1b and c; see also the movie in the Supporting Information). This shows that Rh-PTD has crossed the GUV membranes, which remain intact (Figure 1c). Thus, we see that the membrane transduction activity of Rh-PTD requires the presence of a threshold amount of DOPE in the membrane.

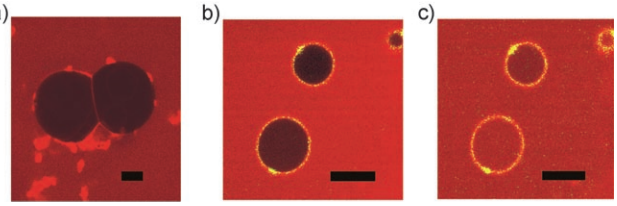

Figure 1. Rhodamine-tagged TAT PTD is applied to the exterior of GUVs of different lipid compositions and the results are imaged by using confocal microscopy. a) Rh-PTD never enters PS/PC 20:80 membranes. b) Less than 3 seconds after addition, Rh-PTD remains mostly exterior to BODIPY-tagged PS/PC/PE (20:40:40) membranes. c) About 30 seconds later, the vesicle interior has the same brightness as the outside, a result showing that the Rh-PTD concentration has equilibrated on both sides of the membrane. Scale bars: 5 μm. BODIPY: 2-(4,4-difluoro-5,7-dimethyl-4-bora-3a,4a-diaza-*s*-indacene-3-pentanoyl)-1-hexadecanoyl-*sn*-glycero-3-phosphocholine; PC: phosphocholine; PE: phosphoethanolamine; PS: phospho-L-serine.

[*] A. Mishra, Dr. V. D. Gordon, L. Yang, Prof. Dr. G. C. L. Wong
Department of Materials Science and Engineering
University of Illinois Urbana Champaign
1304 W. Green St., Urbana, IL 61801 (USA)
Fax: (+1) 217-333-2736
E-mail: gclwong@uiuc.edu
Homepage: http://prometheus.mse.uiuc.edu/
R. Coridan, Prof. Dr. G. C. L. Wong
Department of Physics
University of Illinois Urbana Champaign (USA)

[**] We acknowledge helpful discussions with S. Gruner, J. J. Cheng, and A. Garcia. The work is supported in part by the National Science Foundation (NSF) Division of Materials Research (Grant no.: 0409769), the NSF Nanoscale Science and Engineering Centers, and the National Institutes of Health (Grant no.: 1R21K6843-01). The X-ray diffraction data were collected at the Stanford Synchrotron Radiation Laboratory (Palo Alto, CA; BL4-2) and the Advanced Photon Source (Argonne, IL; BESSRCAT BL-12ID).

Supporting information for this article is available on the WWW under http://www.angewandte.org or from the author.

To elucidate the molecular interactions between the TAT PTD and such PE-rich membranes, we use synchrotron SAXS analysis to study complexes formed by this PTD and DOPS/DOPE (20:80) membranes. Before exposure to TAT PTD, we see a broad form factor (Figure 2a, bottom), as expected for small unilamellar vesicles (SUVs, diameters of 15–50 nm). After exposure to the PTD (at a peptide/lipid (P/L) molar ratio of 1:40), 9 new diffraction peaks are observed (Figure 2a, middle). The peak positions in q show excellent agreement with those expected for a cubic "double diamond" *Pn3m* phase with a lattice constant of $a = 10.97$ nm (Figure 2b). This is a bicontinuous phase characterized by negative Gaussian curvature, threaded with tetrahedral networks of water pores (Figure 2c and d). Its presence indicates that the initial SUVs have undergone a drastic topological transformation.[12,13] The lattice constant indicates that the pores in these structures are ≈6 nm in diameter (Figure 2d). In the presence of 100 mM NaCl, the same peaks are also observed (Figure 2a, top), thereby indicating that this reconstruction can occur at physiological salt concentrations.

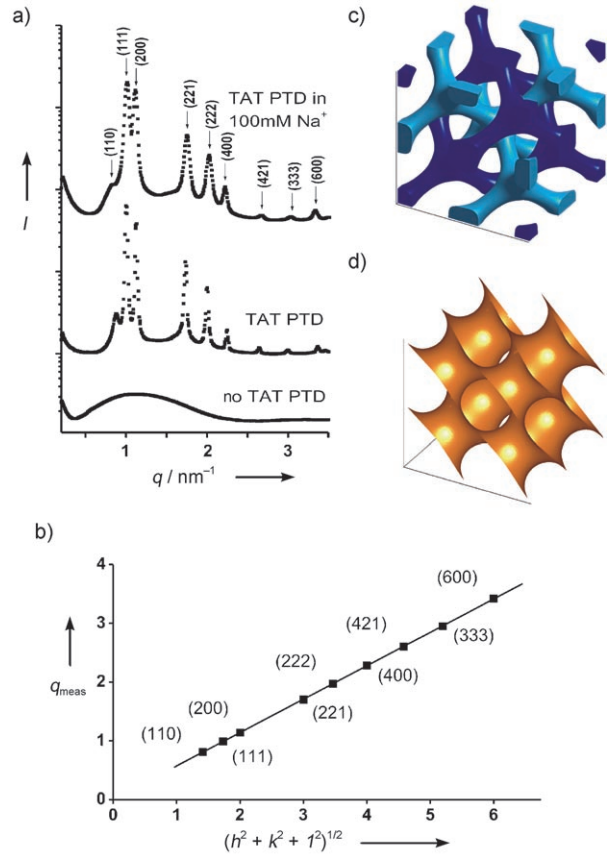

Figure 2. a) SAXS data show that PS/PE (20:80) vesicles (bottom) undergo a topological transformation when complexed with the TAT PTD, to form a cubic "double-diamond" (*Pn3m*) phase with two nonintersecting networks of pores ≈6 nm in diameter (middle). Addition of the TAT PTD in the presence of 100 mM Na^+ results in the same cubic phase (top). b) The agreement between measured peak positions and the corresponding *Pn3m* cubic indexation, $q_{meas} = 2\pi\sqrt{(h^2 + k^2 + l^2)/a}$ (where h, k, and l are the Miller indices and $a = 10.97$ nm is the lattice parameter). Schematic representations of c) the two nonintersecting networks of water pores, and d) the zero-mean-curvature surface at the midplane between the two membrane leaflets.

The effect of the TAT PTD on PE-rich membranes is the generation of negative Gaussian curvature, the type of curvature that characterizes the saddle-shaped surfaces inside the holes of donuts.[15] Our data show that ANTP penetratin,[16] another arginine-rich PTD, also generates negative Gaussian curvature in PE-rich membranes and forms a cubic *Pn3m* phase ($a = 14.1$ nm, data not shown).

Polylysine has the same charge as the TAT PTD but no transduction activity. In complexes formed with polylysine and DOPS/DOPE (20:80) SUVs (P/L ratio of 1:40), SAXS analysis shows 3 diffraction peaks with peak positions at the $1:\sqrt{3}:2$ ratio characteristic of the inverted hexagonal phase (H_{II}; Figure 3a). This structural assignment is confirmed by

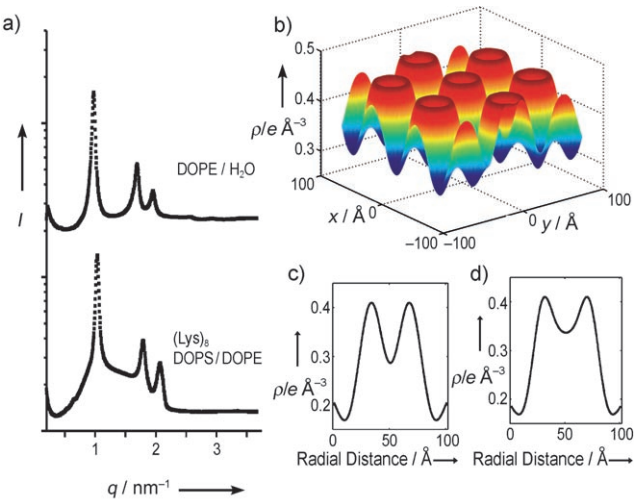

Figure 3. a) SAXS data for polylysine complexed with PS/PE (20:80; bottom) and PE (top) membranes show peak positions that have the characteristic $1:\sqrt{3}:2$ ratio for an inverted hexagonal (H_{II}) phase. b) Electron-density reconstruction for polylysine complexed with PS/PE (20:80) membranes. Radial slices of such reconstructions show that the electron density (ρ) in the H_{II} channels formed when c) polylysine is complexed with DOPS/DOPE (20:80) membranes is lower than that with d) a pure DOPE H_{II} phase.

an electron-density profile of the unit cell (Figure 3b and c), reconstructed from X-ray data through Fourier synthesis.[17] The density profile shows unambiguously that the complex is in an inverted hexagonal H_{II} phase with the small (2.0 nm in diameter) water channels "plugged" by polylysine, thereby allowing the cationic polylysine to charge compensate the anionic DOPS lipid heads. The X-ray experiments above show that the transduction activity of these peptides is correlated to their ability to induce negative Gaussian curvature.

TAT PTD exhibits a hierarchy of peptide–lipid interactions with different lipid species. The cationic PTD interacts strongly with localized negative charges in both anionic *and* neutral zwitterionic lipids (DOPS and DOPC) but does not interact directly with DOPE (see the Supporting Information). To identify the minimum conditions for *Pn3m*

phase formation, we studied the DOPS/DOPE phase diagram as a function of increasing DOPS fraction and P/L ratio. A *Pn3m* cubic phase appears at DOPS fractions of 20–30%, which are typical fractions in eukaryotic membranes (Figure 4a). Moreover, this occurs for a wide range of P/L ratios. Clearly, DOPS, *as well as* DOPE, is necessary for the formation of the *Pn3m* cubic phase. We also systematically

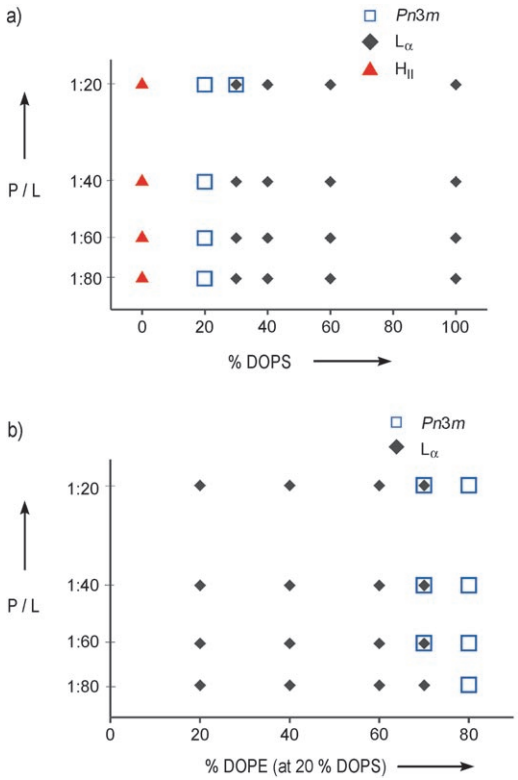

Figure 4. a) The phase diagram of TAT PTD with PS/PE membranes shows that TAT PTD cannot induce pure PE to form the *Pn3m* phase. PS and PE are both necessary for the *Pn3m* cubic phase. L_α: lamellar phase. b) An investigation of self-assembly between TAT PTD with tertiary PS/PE/PC membranes allows us to vary the intrinsic curvature independently of the charge density. The results indicate that a high local concentration of negative curvature lipids such as PE (>70%) is necessary for the *Pn3m* cubic phase.

isolated the effects of membrane curvature by investigating tertiary DOPS/DOPE/DOPC membranes at different P/L ratios. We varied the DOPE/DOPC ratio while keeping the DOPS concentration constant at a typical eukaryotic value of 20%. This varies the intrinsic curvature without significantly changing the charge density. The resultant phase diagram (Figure 4b) shows that a high local concentration of DOPE (70–80%) is necessary for the cubic phase, which can be observed for a wide range of P/L ratios (1:20 to 1:80). For 70% DOPE, coexistence between the lamellar and cubic phases is observed. This is consistent with the observation that TAT PTD requires high DOPE fractions and suggests that TAT can induce phase separation in order to organize the *Pn3m* phase.

We believe that these structural trends in TAT PTD toward pore formation, the hierarchy of interactions implicit in this trend, and the high transduction activity of TAT PTD can be connected with a simple geometric mechanism. Negative Gaussian curvature is needed topologically to form pores. The TAT PTD is observed to generate negative Gaussian curvature, which indicates that it can simultaneously induce positive curvature along one principal direction and negative curvature in the other to make "saddle-shaped" deformations.[15] By contrast, polylysine only generates negative mean curvature by bending the membrane along one direction to make "cylinder-shaped" deformations. These geometric observations combine with the importance of negative-curvature DOPE lipids for the TAT PTD's activity and the hierarchy of PTD–lipid interactions to suggest a possible molecular mechanism for transduction: Strong electrostatic interactions allow polylysine to generate negative curvature in mixtures of anionic and neutral lipids. This can be seen in the tendency for the membrane sheet to wrap the polypeptide in the direction perpendicular to the peptide axis, thereby creating an H_{II} phase. TAT PTD is mostly polyarginine; arginine can form bidentate hydrogen bonds that interact simultaneously with phosphate moieties on multiple lipid headgroups. Lysine can only form monodentate hydrogen bonds that interact with the phosphate moiety on a single headgroup.[18] We speculate that, because of this, arginine groups are more efficient than lysine groups in cross-linking the bulky headgroups of DOPS and DOPC phospholipids. This generates positive curvature along the contour length of the peptide chain in addition to negative curvature perpendicular to it, thereby creating negative Gaussian curvature. The preferential interaction of the TAT PTD with non-PE lipids suggests that these tendencies may be reinforced through local lipid segregation: Repartitioning of DOPE away from the peptide can concentrate negative curvature perpendicular to the peptide axis, as well as enrich the DOPE content of the inner membrane leaflet not in contact with TAT PTD, thereby increasing positive curvature along the peptide axis.

In summary, the transduction activity of TAT PTD correlates with its ability to induce negative Gaussian curvature. Other cationic peptides, like polylysine, are unable to do so and, therefore, do not have significant transduction activity. These results have strong implications for the rational design of cell-penetrating peptides.

Received: September 27, 2007
Revised: November 8, 2007
Published online: March 12, 2008

Keywords: lipids · membranes · peptides · pore formation · transduction

[1] J. S. Wadia, S. F. Dowdy, *Adv. Drug Delivery Rev.* **2005**, *57*, 579.
[2] M. Lewin, N. Carlesso, C. H. Tung, X. W. Tang, D. Cory, D. T. Scadden, R. Weissleder, *Nat. Biotechnol.* **2000**, *18*, 410.
[3] S. R. Schwarze, A. Ho, A. Vocero-Akbani, S. F. Dowdy, *Science* **1999**, *285*, 1569.
[4] E. P. Holowka, V. Z. Sun, D. T. Kamei, T. J. Deming, *Nat. Mater.* **2007**, *6*, 52.

[5] P. A. Wender, D. J. Mitchell, K. Pattabiraman, E. T. Pelkey, L. Steinman, J. B. Rothbard, *Proc. Natl. Acad. Sci. USA* **2000**, *97*, 13003.
[6] J. S. Wadia, R. V. Stan, S. F. Dowdy, *Nat. Med.* **2004**, *10*, 310.
[7] G. C. L. Wong, J. X. Tang, A. Lin, Y. Li, P. A. Janmey, C. R. Safinya, *Science* **2000**, *288*, 2035.
[8] L. Yang, H. Liang, T. E. Angelini, J. Butler, R. Coridan, J. X. Tang, G. C. L. Wong, *Nat. Mater.* **2004**, *3*, 615.
[9] I. Koltover, T. Salditt, J. O. Raedler, C. R. Safinya, *Science* **1998**, *281*, 78.
[10] U. Raviv, D. J. Needleman, Y. Li, H. P. Miller, L. Wilson, C. R. Safinya, *Proc. Natl. Acad. Sci. USA* **2005**, *102*, 11167.
[11] D. J. Mitchell, D. T. Kim, L. Steinman, C. G. Fathman, J. B. Rothbard, *J. Pept. Res.* **2000**, *56*, 318.
[12] E. L. Thomas, D. B. Alward, D. J. Kinning, D. C. Martin, *Macromolecules* **1986**, *19*, 2197.
[13] P. T. C. So, S. M. Gruner, S. Erramilli, *Phys. Rev. Lett.* **1993**, *70*, 3455.
[14] P. Garstecki, R. Holyst, *Phys. Rev. E* **2001**, *64*, 021501.
[15] A. Ben-Shaul, W. M. Gelbart in *Micelles, Membranes, Microemulsions and Monolayers* (Eds.: W. M. Gelbart, A. Ben-Shaul, D. Roux), Springer, New York, **1994**, pp. 1–104.
[16] D. Derossi, A. H. Joliot, G. Chassaing, A. Prochiantz, *J. Biol. Chem.* **1994**, *269*, 10444.
[17] D. C. Turner, S. M. Gruner, *Biochemistry* **1992**, *31*, 1340.
[18] J. B. Rothbard, T. C. Jessop, P. A. Wender, *Adv. Drug Delivery Rev.* **2005**, *57*, 495.

